Kinetics of Nanoparticles Formation Under UV, VIS and IR Nanosecond Laser Irradiation of a Silver-Ions-Enriched Glass

Ekaterina Babich[*1,2], Vladimir Kaasik[1,2], Igor Reduto[3], Sergey Scherbak[1,2,4], and Andrey Lipovskii[1,2]

[1]*Peter the Great St. Petersburg Polytechnic University, St. Petersburg, Russia*
[2]*Alferov University, St. Petersburg, Russia*
[3]*University of Eastern Finland, Joensuu, Finland*
[4]*Higher School of Economics, St. Petersburg, Russia*
[*]*Corresponding author's e-mail: babich.katherina@gmail.com*

We reveal the impact of wavelength and energy of a nanosecond laser irradiation on the formation of silver nanoparticles in soda-lime glass enriched with silver ions. Optical extinction spectra, atomic force microscope images and surface profiles of the laser-modified regions of the glass are compared for laser irradiations at 1.06, 0.53 and 0.35 μm wavelength in 7-13 J/cm^2 laser fluence range. The evolution of nanoparticles' radius, concentration and size distribution is deduced from optical extinction spectra and supported by Mie-scattering calculations and by experimental characterizations. It is shown that 1) used laser fluencies independently on the wavelengths provide formation of nanoparticles in subsurface glass layer; 2) decrease in the wavelength intensifies glass sputtering and partial removal of formed nanoparticles; 3) the increase in the fluence leads to the formation of higher number of smaller nanoparticles.
DOI: 10.2961/jlmn.2021.02.2003
Keywords: soda-lime glass, ion-exchange, silver, nanoparticles, nanosecond laser

1. Introduction

Glasses containing silver nanoparticles (NPs) in the bulk and on the surface are of interest due to plasmonic properties of the NPs, which, in particular, provide high and fast optical nonlinearity [1], enhancement of Raman scattering [2], strong catalytic capability and selective toxicity [3,4], and modification of luminescent characteristics of doped glasses [5]. Applications of glasses with silver NPs include sensing, catalysis, biomedicine and other usage (see [3,6] and references therein). To exploit these properties, in most cases, NPs need to be formed on the glass surface or in the immediate vicinity of it. Thus, methods to create these structures are required. In principle, NPs can be either deposited/formed on the glass surface using external source [7] or formed via processing of silver-containing glass [8]. The latter approach looks preferable, for it allows obtaining NPs both in the bulk and on the surface of glasses. Moreover, NPs grow on the surface via silver out-diffusion from the bulk of the glass and, therefore, they have better adhesion.

Laser modification of silver containing which allows fabricating given 2D patterns of NPs in glasses was reported in 2000th [9–11], and, later, continuous UV and blue lasers [12–14] and pulsed visible [15,16], IR [3,17,18] and UV [19–21] lasers with high laser fluence were successfully used. Formation of silver NPs under laser irradiation goes through the reduction of silver ions and their diffusion-driven clustering followed by the growth of the NPs. The process of silver reduction is two-fold: because of plain heating of the glass by absorbed irradiation (this works similarly to the reduction of silver ions in thermally heated glasses [21]) and through photoexcitation of electrons (at longer wavelength through multiphoton absorption/avalanche ionization) followed by the reaction $Ag^+ + e^- \rightarrow Ag^0$ [15]. While the formation of NPs via nanosecond laser irradiation of silver-ions-enriched glasses was demonstrated several times, no direct comparison of the kinetics of silver NPs formation under different laser wavelength was presented. This is important because different applications require different properties of NPs, which can be adjusted in fabrication. This study aimed to reveal the impact of nanosecond laser wavelength choice and fluence on the properties of silver NPs formed via irradiation of silver-ions-enriched glasses.

2. Materials and Methods

We used a 1 mm-thick soda-lime silicate glass slide [22] containing 14.3 wt.% of sodium oxide as a host for silver ions, the ions being introduced in the glass by $Ag^+ \leftrightarrow Na^+$ ion-exchange procedure. Particularly, the slide was immersed into the melt of $(AgNO_3)_{5wt.\%}(NaNO_3)_{95wt.\%}$ at 325° C for 20 min. In the course of the ion-exchange, silver ions from the melt replaced more than 70% of sodium ions in the subsurface glass layer and the maximal penetration depth of silver ions was ~7 μm [23].

The glass enriched with silver ions was irradiated with Nd:YAG laser (Litron Nano L) at 1.06, 0.53 and 0.35 μm wavelength using different laser fluencies. The laser provided 6 ns-long pulses. The laser beam was focused on the glass surface to a spot of ~250, 160 and 90 μm in diameter for 1.06, 0.53 and 0.35 μm wavelengths, respectively. We used the computer-driven platform (Thorlabs MT3/M-Z8 3D) to move the glass slide in the plane perpendicular to the laser beam at the speed of 200 μm/s. The pulse repetition rate was chosen for each laser wavelength in such a way that the laser pulses

partially overlaped on the glass surface. We measured the laser energy by pyroelectric joulemeter (Standa 11QE12LP-S-MB) and kept the laser fluence at the same level for all the wavelengths used. The parameters of the irradiation are presented in Table 1.

Table 1. Parameters of laser irradiation

Laser wavelength (μm)	Laser fluence (J/cm^2)	Frequency (Hz)
0.35	7 – 11.5	3
0.53	9 – 12.5	2
1.06	10 – 13	2

After the irradiation, the surface of the glass was characterized using stylus profilometer (Bruker DektakXT), scanning electron microscope (SEM LEO 1550 Gemini) and atomic force microscope (AFM Bruker ICON). For the latter we used ScanAsyst AFM tips having nominal curvature of 2 nm.

The irradiation led to yellow coloration of the glass (indicating formation of silver NPs) for all the wavelengths and fluencies used. To characterize NPs we measured optical extinction spectra in the irradiated regions using a homemade setup that included a halogen lamp (Ocean Optics HL-2000-FHSA-LL) as a light source and a modular spectrometer (Solar LS SC82) as a detector. The illumination and collection light spots coincided in size, being ~240 μm in diameter. We also made X-ray diffractometry (XRD) analysis (D8 Discover (Cu Kα)) of the irradiated glass. Note, XRD analysis required area of interest to be at least 1x1cm^2, therefore we made separate sample irradiated with 0.35 μm laser at 0.3 J/cm^2 fluence, the laser beam speed and pulse repetition rate being 1mm/s and 80 kHz, respectively.

We used MieLab [24] and COMSOL Multiphysics programs to calculate extinction spectra of spherical silver NPs embedded in glass. In calculations we used Johnson and Cristy's dispersion of silver [25], glass index 1.5 and assumed that NPs size distribution is a normal one. The comparison of calculated and measured spectra allowed us to evaluate NPs size, concentration and polydispersity.

To estimate the thickness of the subsurface glass layer containing silver nanoparticles we additionally performed reactive ion etching (RIE Plasmalab System 80) followed by SEM and optical characterization of the sample. In RIE we used CHF_3 and Ar with the gas flows of 12 and 38 sccm, respectively, the base pressure of 43 mTorr, and the RF power was 220 W.

3. Results and Discussion

In Fig. 1 a and b one can see the appearance of craters on the irradiated glass surface, and yellow coloration of the glass at the periphery of the craters (colored "rings"), respectively. The brightest coloration is observed after the irradiation at 1.06 μm, while the deepest craters are formed after the irradiation at 0.35 μm. XRD of the glass irradiated at 0.35 μm (see Section 2) evidences the presence of crystalline silver (Fig. 1c): the detected peaks are assigned to diffraction from the (111), (200), (220), (311) and (222) planes of silver.

Optical extinction spectra collected in the colored regions of the irradiated glass demonstrate the presence of a resonance at ~450 nm wavelength (see Fig. 1d), which spectral position corresponds to the position of surface plasmon resonance (SPR) of silver NPs [8]. It is known, silver NPs form in the glass under laser irradiation as a result of the agglomeration of silver atoms appearing via the reaction $Ag^+ + e^- \rightarrow Ag^0$ [15]. Silver ions appear via breaking Ag-O bonds in the strongly heated glass [26–28]. The electrons participated

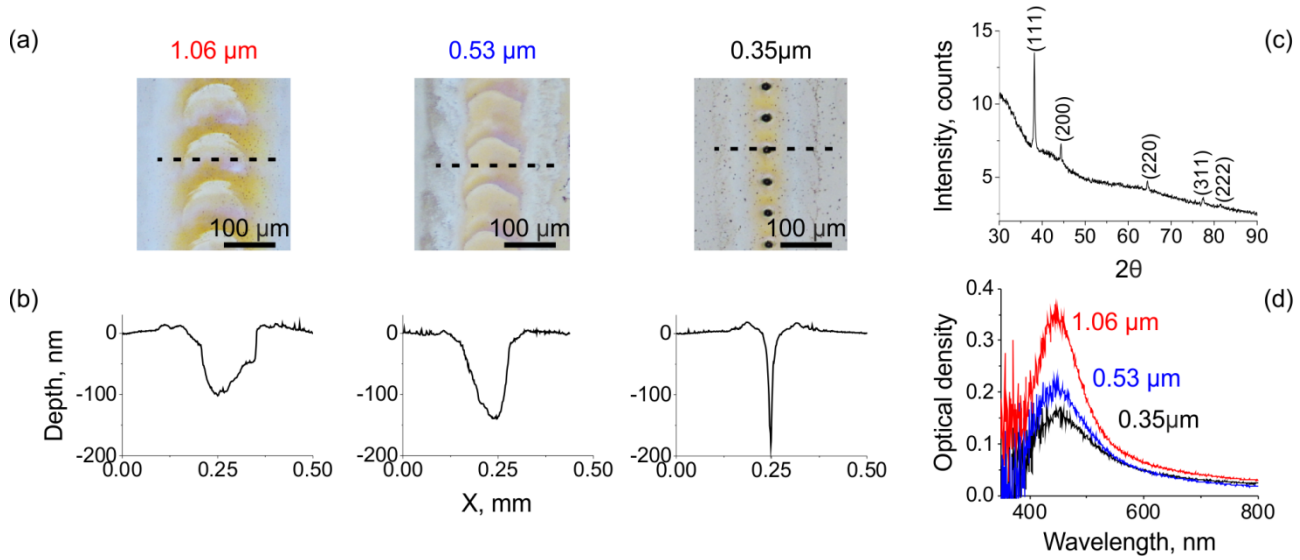

Fig. 1 Typical micrographs (a), surface profiles (b), XRD with denoted crystalline planes of silver corresponding to the observed diffraction peaks (c) and optical extinction spectra (d) of the silver-ions-enriched glass irradiated with ns-laser at 1.06, 0.53 and 0.35 μm wavelengths. The dashed outlines in micrographs indicate where the profilometer scanning was made.

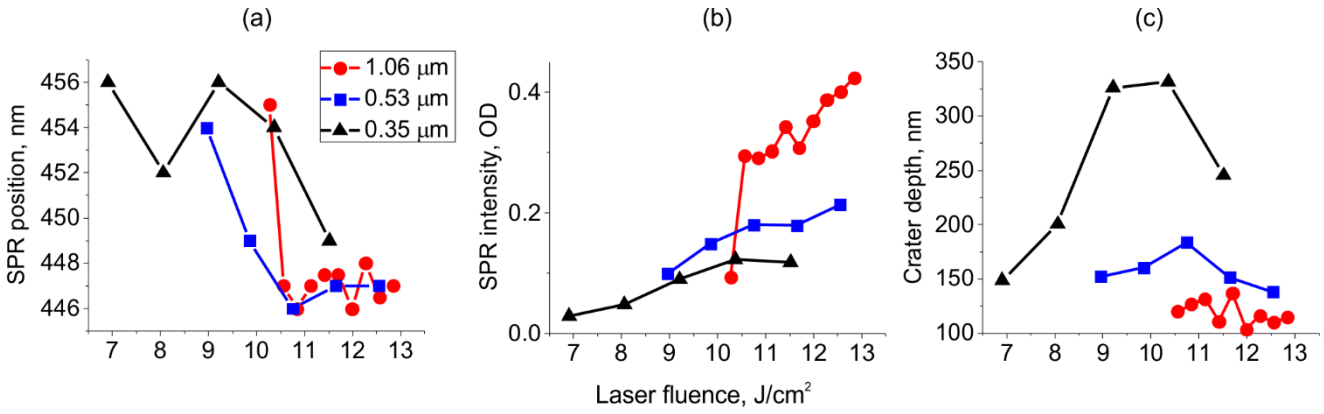

Fig. 2 Surface plasmon resonance spectral position (a) and intensity (b), and crater depth (c) for different wavelengths and laser fluencies of ns-laser irradiation of silver-ions-enriched glass.

in this reaction can be released by non-bridging oxygen atoms [29] or generated through multiphoton absorption or avalanche ionization [30]. Additionally, silver reduction in glasses can occur in heated glasses in the case of water/hydrogen presence [8,31]. The laser irradiation results in heating, melting and partial ablation of the glass, which cause craters and surrounding rims (due surface flux of the glass from the created region in temperature gradient [27]) formation on the glass surface. Thus, the rims are formed from melted glass which went out from the crater zone and partly by the redeposited products from the ablation plume. As demonstrated in Fig. 1, kinetic of NPs formation depends on laser wavelength and fluence. To study this kinetic we obtained the dependencies of the SPR position and intensity and also the crater depth on the laser wavelength and fluence, Fig. 2.

Fig. 2 shows that the decrease in the laser wavelength from 1.06 to 0.35 μm results in weakening of plasmon resonance and deeper craters that evidences intense glass

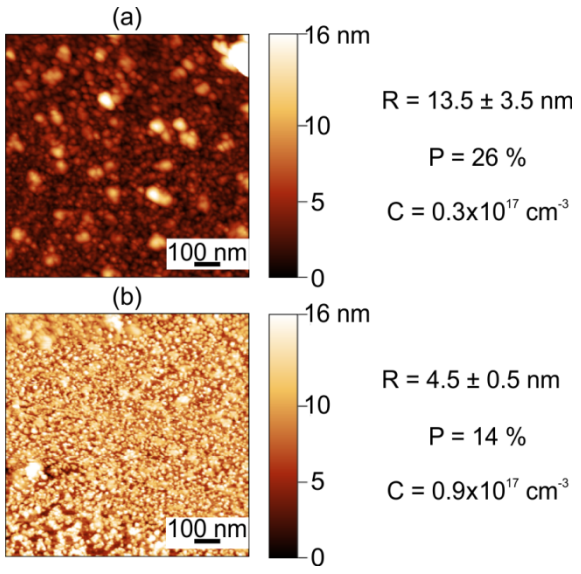

Fig. 3 AFM images of the silver-ions-enriched glass irradiated with ns-laser at 0.35 μm wavelength at (a) 8 J/cm^2 and (b) 10.5 J/cm^2 laser fluence. Average radius, R, and concentration, C, of nanoparticles and polydispersity, P, of their ensemble are denoted.

sputtering and decreasing number of NPs formed by the laser pulse at the crater periphery (the rim region). Indeed, 0.35 μm irradiation falls in the absorption edge of soda-lime glass, and optical density (absorption) of the ion-exchanged glass at this wavelength increases twice compared to 1.06 and 0.53 μm. This results in fastest formation of the ablation plume. The plume, when formed, effectively absorbs laser radiation during the pulse [32], the shorter is the wavelength the stronger is the absorption. At the periphery of the craters reduction of silver ions and clustering of silver atoms with the formation of NPs occur. Firstly, silver nanoislands grow on the glass surface [26], for it is the strongest sink for silver atoms reduced in the most defective and partially leached surface glass layer. Light absorption (the tail of Gaussian light distribution) by these nanoislands during the laser pulse results in their fast heating and transfer the heat to the glass beneath. Taking heat diffusivity in the glass D~$3\cdot10^{-7}$ m^2/s [33] the heat penetration depth in the glass, h~sqrt($D\tau$), during the pulse (τ=6 ns) should be ~40 nm. Since the additional absorption starts after the nanoislands are formed, the effective τ should be less, and 40 nm is the upper estimation. Finally, the nanoparticles should form during the pulse in the heated subsurface region of the glass which is thinner than 40 nm. Better screening the glass by intensive ablation plume arising at shorter irradiation wavelengths results in less effective formation of the NPs nuclei and, respectively in bigger and less numerous NPS, which corresponds to the data presented in Fig. 2. Stronger laser fluence results in more effective nucleation of the NPs [34] and respectively, higher number of smaller nanoparticles. In fact, we observed that under higher fluence the spectral position of SPR shifted towards shorter wavelength, which is typical for smaller NPs, while SPR intensity corresponded to increased number of NPs.

To verify the formation of smaller NPs under increased laser fluence we analyzed AFM images of the glass surface irradiated at 8 J/cm^2 and 10.5 J/cm^2 laser fluencies, both at 0.35 μm wavelength. The scanning was made in the colored regions between craters (see Fig. 1a) and obtained images are presented in Fig. 3. Statistical analysis of the AFM images was made using ImageJ

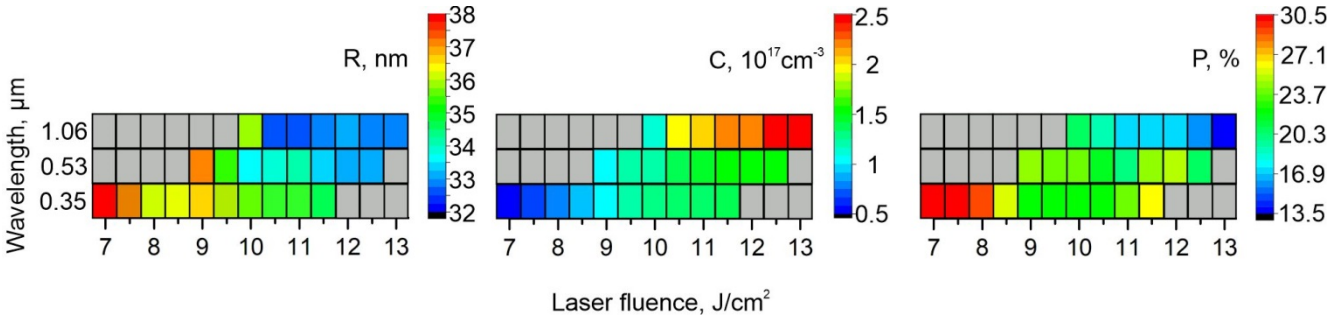

Fig. 4 The maps of average radius, R, concentration, C, of silver nanoparticles and polydispersity, P, of their ensemble plotted in laser wavelength-laser fluence coordinates. The data are retrieved from optical extinction spectra using Mie-scattering calculations.

software [35]: a radius of disc with the same projected area as a nanoparticle was calculated, and retrieved radius distribution was approximated by normal one, from which the polydispersity, P, and average radius, R, of NPs were determined (denoted in Fig. 3). To evaluate volume concentration of NPs, C, we estimated the thickness of the glass layer containing NPs. Reactive ion etching (see details in Section 2) of the glass followed by spectral measurements has shown that the removal of 20 nm surface glass layer resulted in drastic decrease of the SPR absorption amplitude. Moreover, SEM characterization of the etched glass demonstrated barely any NPs on the surface. Thus, we estimated that the layer containing NPs is about 20 nm thick (the half of estimated depth of 40 nm) and calculated the volume concentration of NPs by the division of surface concentration retrieved from AFM images by 20 nm. The AFM images and obtained statistical data (average radius, concentration and polydispersity of NPs) clearly evidence the formation of smaller NPs at higher laser fluence, which corresponds to SPR spectral position and its intensity behavior.

However, we encountered difficulties in studying glass irradiated with a laser at wavelengths of 1.06 and 0.53 μm using AFM and SEM, which did not allow observing NPs on the glass surface. This was due to the high surface roughness of the laser-irradiated glass region (supposedly by the redeposition of some products from the ablation plume) and its low conductivity, respectively. Coating the samples with a 5 nm layer of gold to improve the conductivity and increase the SEM contrast led to the formation of a percolated gold film on the rough glass surface, which also made it impossible to identify silver NPs among gold nanostructures. This situation is consistent with the results of our previous work [36], where we showed that infrared laser irradiation of silver ions-enriched glass leads to the formation of NPs under a thin glass layer. We are sure that this also applies to 0.53 μm laser radiation. We also believe that the direct characterization of the formed NPs is difficult precisely for this reason. Therefore, to compare the influence of the laser wavelength on the formation of NPs and follow the evolution of their size, size distribution, and concentration when laser fluence varied, we analyzed in details optical extinction spectra of the irradiated glass regions.

It is known, spectral position of SPR depends on size and shape of NPs and on dielectric constant of the environment, while the intensity of SPR corresponds mostly to the number of NPs. The observed shift of SPR spectral position cannot be associated with the change in the refractive index of the surrounding medium (glass) because induced by laser heating change in the glass refractive index is of order of one thousandth [37]. Moreover, one should account that AFM images shown in Fig. 3 and performed studies [38–40] indicate the formation of spherical NPs under the laser irradiation of ion-exchanged glasses; therefore, one should not expect SPR shift caused by the influence of the particles shape. Thus, the observed spectral shift of SPR position should be predominantly governed by the size of NPs. In this case, the size, concentration and polydispersity of the NPs can be estimated from optical extinction spectra. We did this using analytical Mie theory calculations [24]. We fitted the calculated spectra to the experimental ones (see Section 2 for details) using NPs radius, concentration and polydispersity as fitting parameters. The obtained values of fitting parameters are presented in Fig. 4.

One can see in Fig. 4 that estimated concentration and polydispersity are in a good agreement with NPs characterization data, while the calculated average radius of NPs is higher than one retrieved from AFM images (see Fig. 3). For example, the optical extinction spectrum of the glass irradiated at 0.35 μm wavelength with 8 J/cm^2 laser fluence demonstrates SPR at ~450 nm. Thus, the Mie calculation predicts that a single nanoparticle needs to be 32 nm in radius to have the same resonant wavelength. However, the NPs radius distribution obtained from the AFM image of this sample (Fig. 3a) show that the average radius is 13.5 ± 3.5 nm.

We believe, the discrepancy in nanoparticles' radius is because Mie calculations in accordance with Ref. 24 do not account for interaction of neighboring NPs. It is known that this interaction can result in a long-wavelength shift of the SPR [41–43]. To estimate influence of interparticle interaction on SPR spectral position we calculated extinction spectra of paired silver nanospheres using COMSOL Multiphysics environment. In calculations we considered only a light polarization vector directed along an interparticle axis because perpendicular configuration is characterized by weaker interaction [43]. From AFM image in Fig. 3a we obtained minimum, maximum and average gaps between the particles: 1, 31 and 7 ± 1 nm, respectively. In Fig. 5 we demonstrate calculated extinction spectra for a single nanoparticle with radius 32 nm and two NPs with radius 13.5 nm separated by these

gaps. One can see, the decrease in the gap from 31 to 1 nm results in long-wavelength shift of the SPR up to 140 nm, and SPR position at ~450 nm corresponds to either single nanoparticle with the radius 32 nm or two 13.5 nm NPs separated by about 7 nm gap. Thus, the discrepancy of AFM and spectral measurements is most probably due to the interaction of NPs. Note that considered two-particles interaction does not exactly correspond to multiparticle effects in a dense film, but nonetheless gives a qualitative understanding about the influence of NPs interaction.

Overall, regularities revealed by performed modeling correspond well with the ones observed experimentally and allow describing kinetics of the NPs formation as the next. The increase in the laser fluence results in formation of higher number of smaller NPs, which size dispersion is lower at high laser fluence at all the wavelengths. Intense laser irradiation generates higher number of electrons and, correspondingly, higher number of nucleation centers of NPs. The decrease of both average radius of NPs and their polydispersity with the increase of laser fluence evidence these for all the wavelengths. Maximal number of NPs forms in the glass under the irradiation at 1.06 μm wavelength, while minimal - at 0.35 μm. As we discussed above, the essential and earlier started absorption by the ablation plume at 0.35 μm wavelength screens the laser radiation, and this results in decreasing number of NPs nuclei. However, the NPs formed under 0.35 μm wavelength are bigger compared to ones formed at 1.06 and 0.53 μm irradiation by the same reason.

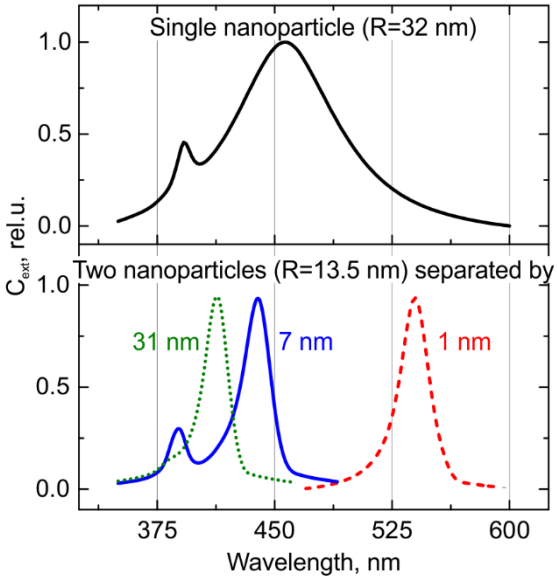

Fig. 5 Calculated normalized extinction cross-section, C_{ext}, for single nanoparticle with radius 32 nm and two nanoparticles with radius 13.5 nm separated by 1, 7 and 31 nm gaps.

It is worth to note that the formation of NPs in the silver enriched glass under high laser fluence essentially differs from one reported by Heinz and co-authors [44], who irradiated a similar glass with about 10 times less UV-laser fluence and obtained ~2 μm thick NPs-containing layer. In their experiment the irradiation intensity was supposedly the ablation threshold, and the shorter wavelength of used excimer laser generated more defects in the glass. Thus, we believe that the formation of NPs in glass in our experiment and in experiments described in [44] occurs differently. We relate this difference to the absence of ablation plume which transversal size exceeds the crater width [32] and which optical absorption in the case of nanosecond pulses during the pulse essentially influences the process under consideration [32]. It should be mentioned that formation of NPs from the ablation plume is also well known [32,45–47], but pure metal target are mainly used for this, and size of the NPs is usually smaller. Thus, in the experiments described above, we consider the formation of NPs from the ablation plume to be much less probable.

4. Conclusions

Irradiation of the soda-lime glass enriched with silver ions with 1.06, 0.53 and 0.35 μm nanosecond laser at 7-13 J/cm^2 laser fluence results in the formation of silver nanoparticles in very thin subsurface glass layer. The decrease in the laser wavelength leads to the intense ablation plume due to efficient absorption of shorter wavelength by the glass The increase of the laser fluence for all the wavelengths results in the formation of higher number of smaller silver nanoparticles due to increasing number of NPs nuclei. Thus, one can control size and number of silver nanoparticles formed in soda-lime glasses under nanosecond laser irradiation by proper choice of laser wavelength and energy.

Acknowledgments

E.B. thanks the Council for Grants of the President of the Russian Federation (project SP-1491.2021.4). V.K., S.Sch. and A.L. thank the Ministry of Science and Higher Education of the Russian Federation (project # FSRM-2020-001). I.R. thanks the Academy of Finland Mobility Grant, and Academy of Finland Flagship PREIN, and A.L. thanks the Academy of Finland Grant # 323052.

References

[1] Y.X. Zhang, and Y.H. Wang: RSC Adv., 7, (2017) 45129.
[2] M.T. Yaraki, and Y.N. Tan: Chem. – An Asian J., 15, (2020) 3180.
[3] A.A. Menazea, and A.M. Abdelghany: Radiat. Phys. Chem., 174, (2020) 108958.
[4] S. Pandey, J.Y. Do, J. Kim, and M. Kang: Carbohydr. Polym., 230, (2020) 115597.
[5] S. Stanek, P. Nekvindova, B. Svecova, S. Vytykacova, M. Mika, J. Oswald, O. Barkman, and J. Spirkova: Opt. Mater. (Amst)., 72, (2017) 183.
[6] S. Berneschi, G.C. Righini, and S. Pelli: Appl. Sci., 11, (2021) 4610.
[7] M. Pišlová, K. Kolářová, B. Vokatá, A. Brož, P. Ulbrich, L. Bačáková, Z. Kolská, and V. Švorčík: Mater. Sci. Eng. C., 115, (2020) 111087.
[8] M. Pišlová, K. Kolářová, B. Vokatá, A. Brož, P. Ulbrich, L. Bačáková, Z. Kolská, and V. Švorčík: Mater. Sci. Eng. C., 115, (2020) 111087.
[9] J.R. Salgueiro, V. Moreno, and J. Linares: Proc. SPIE., 3936, (2000) 164.
[10] I. Antonov, F. Bass, Y. Kaganovskii, M. Rosenbluh, and A. Lipovskii: J. Appl. Phys., 93, (2003) 2343.

[11] A. Miotello, M. Bonelli, G. De Marchi, G. Mattei, P. Mazzoldi, C. Sada, and F. Gonella: Appl. Phys. Lett., 79, (2001) 2456.
[12] M.D. Niry, J. Mostafavi-Amjad, H.R. Khalesifard, A. Ahangary, and Y. Azizian-Kalandaragh: J. Appl. Phys., 111, (2012) 033111.
[13] T. Tite, N. Ollier, M.C. Sow, F. Vocanson, and F. Goutaland: Sensors Actuators, B Chem., 242, (2017) 127.
[14] F. Goutaland, M. Sow, N. Ollier, and F. Vocanson: Opt. Mater. Express., 2, (2012) 350.
[15] J.P. Blondeau, S. Pellerin, V. Vial, K. Dzierzęga, N. Pellerin, and C. Andreazza-Vignolle: J. Cryst. Growth., 311, (2008) 172.
[16] O. Véron, J. P. Blondeau, M. Grabiec, A. Wolak, K. Dzierżęga, N. Ollier, F. Goutaland, M.C. Sow, S. Pellerin, and N. Pellerin: Plasmonics, 8, (2013) 93.
[17] A.A. Menazea, A.M. Abdelghany, W.H. Osman, N.A. Hakeem, and F.H. Abd El-Kader: J. Non. Cryst. Solids., 513, (2019) 49.
[18] V.I. Egorov, I.V. Zvyagin, D.A. Klyukin, and A.I. Sidorov: J. Opt. Technol., 81, (2014) 270.
[19] I. Reduto, S. Wackerow, S. Zolotovskaya, A. Abdolvand, A. Lipovskii, and Y. Svirko: J. Phys. Conf. Ser., 1461, (2020) 012136.
[20] S. Wackerow, and A. Abdolvand: Opt. Express., 22, (2014) 5076.
[21] J. Zhang, W. Dong, J. Sheng, J. Zheng, J. Li, L. Qiao, and L. Jiang: J. Cryst. Growth., 310, (2008) 234.
[22] Agar Scientific, Microscope slides, (2021). www.agarscientific.com/microscope-slides.html (accessed June 08, 2021).
[23] V.V. Zhurikhina, M.I. Petrov, K.S. Sokolov, and O.V. Shustova: Tech. Phys., 55, (2010) 1447.
[24] O. Peña-Rodríguez, P.P. González Pérez, and U. Pal: Int. J. Spectrosc., 2011, (2011) 1.
[25] P.B. Johnson, and R.W. Christy: Phys. Rev. B., 6, (1972) 4370.
[26] A. Redkov, S. Chervinskii, A. Baklanov, I. Reduto, V. Zhurikhina, and A. Lipovskii: Nanoscale Res. Lett., 9, (2014) 1.
[27] M. Rosenbluh, I. Antonov, D. Ianetz, Y. Kaganovskii, and A.A. Lipovskii: Opt. Mater., 24, (2003) 401.
[28] T. Delgado, D. Nieto, and M.T. Flores-Arias: Opt. Lasers Eng., 86, (2016) 29.
[29] V. Rastogi, S. Chaurasia, and D.S. Munda: J. Non. Cryst. Solids., 463, (2017) 138.
[30] D. Nieto, J. Arines, G.M. O'Connor, and M.T. Flores-Arias: Appl. Opt., 54, (2015) 8596.
[31] A. Miotello, G. De Marchi, G. Mattei, and P. Mazzoldi: Appl. Phys. A Mater. Sci. Process., 67, (1998) 527.
[32] K.W. Kolasinski, M.C. Gupta, and L.V. Zhigilei: "Plume and Nanoparticle Formation During Laser Ablation" in "Encyclopedia of Interfacial Chemistry: Surface Science and Electrochemistry" ed. by K. Wandelt, (Elsevier, 2018) p.594.
[33] R.W. Hopper, and D.R. Uhlmann: J. Appl. Phys., 41, (1970) 4023.
[34] E. Cattaruzza, M. Mardegan, E. Trave, G. Battaglin, P. Calvelli, F. Enrichi, and F. Gonella: Appl. Surf. Sci., 257, (2011) 5434.
[35] ImageJ®, ImageJ, (2021). www.imagej.net (accessed June 08, 2021).
[36] E. Babich, V. Kaasik, A. Redkov, T. Maurer, and A. Lipovskii: Nanomaterials, 10, (2020) 1849.
[37] S.G. Demos, B.N. Hoffman, C.W. Carr, D.A. Cross, R.A. Negres, and J.D. Bude: Opt. Express., 27, (2019) 9975.
[38] M. Grabiec, A. Wolak, O. Véron, J.P. Blondeau, N. Pellerin, M. Allix, S. Pellerin, and K. Dzierzega: Plasmonics, 7, (2012) 279.
[39] N. Nedyalkov, N.E. Stankova, M.E. Koleva, R. Nikov, M. Grozeva, E. Iordanova, G. Yankov, L. Aleksandrov, R. Iordanova, and D. Karashanova: Opt. Mater. (Amst)., 75, (2018) 646.
[40] A.A. Menazea, A.M. Abdelghany, N.A. Hakeem, W.H. Osman, and F.H. Abd El-Kader: J. Electron. Mater., 49, (2020) 826.
[41] N. Hooshmand, and M.A. El-Sayed: Proc. Natl. Acad. Sci. U. S. A., 116, (2019) 19299.
[42] E.S. Babich, S.A. Scherbak, A.V. Redkov, A.N. Kamenskii, I.V. Reduto, and A.A. Lipovskii: J. Nanophotonics., 11, (2017) 032503.
[43] W. Rechberger, A. Hohenau, A. Leitner, J.R. Krenn, B. Lamprecht, and F.R. Aussenegg: Opt. Commun., 220, (2003) 137.
[44] M. Heinz, V.V. Srabionyan, A.L. Bugaev, V.V. Pryadchenko, E.V. Ishenko, L.A. Avakyan, Y.V. Zubavichus, J. Ihlemann, J. Meinertz, E. Pippel, M. Dubiel, and L.A. Bugaev: J. Alloys Compd., 681, (2016) 307.
[45] T. Takiya, and N. Fukuda: "Nanoparticle Formation and Deposition by Pulsed Laser Ablation" in "Practical Applications of Laser Ablation" ed by D. Yang, (IntechOpen, 2021) p.205.
[46] M. Kim, S. Osone, T. Kim, H. Higashi, and T. Seto: KONA Powder Part. J., 34, (2017) 80.
[47] D. Batani, T. Vinci, and D. Bleiner: Laser Part. Beams, 32, (2014) 1.

(Received: June 9, 2021, Accepted: September 11, 2021)